# Quantum Antireflection Temporal Coatings: Quantum State Frequency Shifting and Inhibited Thermal Noise Amplification

Iñigo Liberal,* J. Enrique Vázquez-Lozano, and Victor Pacheco-Peña

The quantum optical response of antireflection temporal coatings (ATCs), that is, matching temporal layers that suppress the generation of backward waves in temporal boundaries, is investigated. The results reveal that quantum ATCs are characterized for inducing a frequency shift of the quantum state, while preserving all photon statistics intact. Thus, they can find application for fast quantum frequency shifting in photonic quantum networks. The quantum theory also provides additional insight on their classical mode of operation, clarifying which quantities are preserved through the temporal boundary. Last, it is shown that quantum ATCs allow for fast temporal switching without amplification of thermal fields.

## 1. Introduction

Temporal metamaterials (materials with a designed temporal variation of their constitutive parameters) provide an additional and fundamentally different degree of freedom in engineering light–matter interactions.[1–5] The elementary constituent of temporal metamaterials is the temporal boundary, that is, the rapid change in time of the material parameters of the system.[6,7] The main signature of a temporal boundary is the generation of forward and backward waves (temporal equivalent of transmitted and reflected signal at a spatial boundary between two media), shifted in frequency, but preserving the wavenumber in order to enforce the continuity of the *D* and *B* fields.[6–9]

I. Liberal, J. E. Vázquez-Lozano
Department of Electrical
Electronic and Communications Engineering
Institute of Smart Cities (ISC)
Public University of Navarre (UPNA)
Pamplona 31006, Spain
E-mail: inigo.liberal@unavarra.es
V. Pacheco-Peña
School of Mathematics
Statistics and Physics
Newcastle University
Newcastle Upon Tyne NE1 7RU, UK

As the generation of a backward wave can be undesired in many practical scenarios, antireflection temporal coatings (ATCs) have recently emerged as a design strategy to achieve reflection-less temporal boundaries.[10] Inspired by the design of spatial matching layers,[11] temporal slabs can be tailored such that destructive interference inhibits the generation of a backward wave. At the same time, given that spatial interfaces and temporal boundaries have different properties, spatial and temporal matching layers also present different features, as discussed in refs. [12–14]. The extension to multilayered temporal sequences enables a finer control over the spectral response of ATCs. Several approaches have pushed forward this concept, leveraging strategies from advanced filter design,[15] granting access to higher-order functions,[14] and enabling ultrawideband pulse operation.[16]

The quantum theory of time-varying media provides a more complete description of the associated optical processes. It provides not only a description in terms of energy and field amplitudes but also grants full access to the information encoded in the quantum state of the electromagnetic field, including photon production and absorption processes, as well as changes in quantum correlations.[17,18] Analyzing the quantum response of time-varying media extends their scope to new applications, including basic research on vacuum amplification effects,[19,20] as well as the development of new amplification schemes[21] and light sources for quantum technologies.[22,23]

Building upon this ground, in this work, we investigate the quantum response of ATC; hereafter, referred to as quantum ATCs. As we will show, the quantum theory provides additional physical insight on their classical mode of operation. Moreover, it points toward additional potential applications of ATCs such as quantum frequency shifting and fast switching while inhibiting the amplification of thermal fields.

The first experimental demonstration of a temporal boundary and a temporal slab with zero backward wave features was recently reported based on transmission line metamaterials operating at radio frequencies.[24] Time crystals exhibiting a momentum band-gap have also been demonstrated at microwave frequencies with transmission line metamaterials loaded with varactors.[25] In this sense, we expect that our theoretical results on thermal noise amplification/suppression could be tested on those platforms. Further, a promising system for testing our

**ADVANCED
SCIENCE NEWS**

www.advancedsciencenews.com
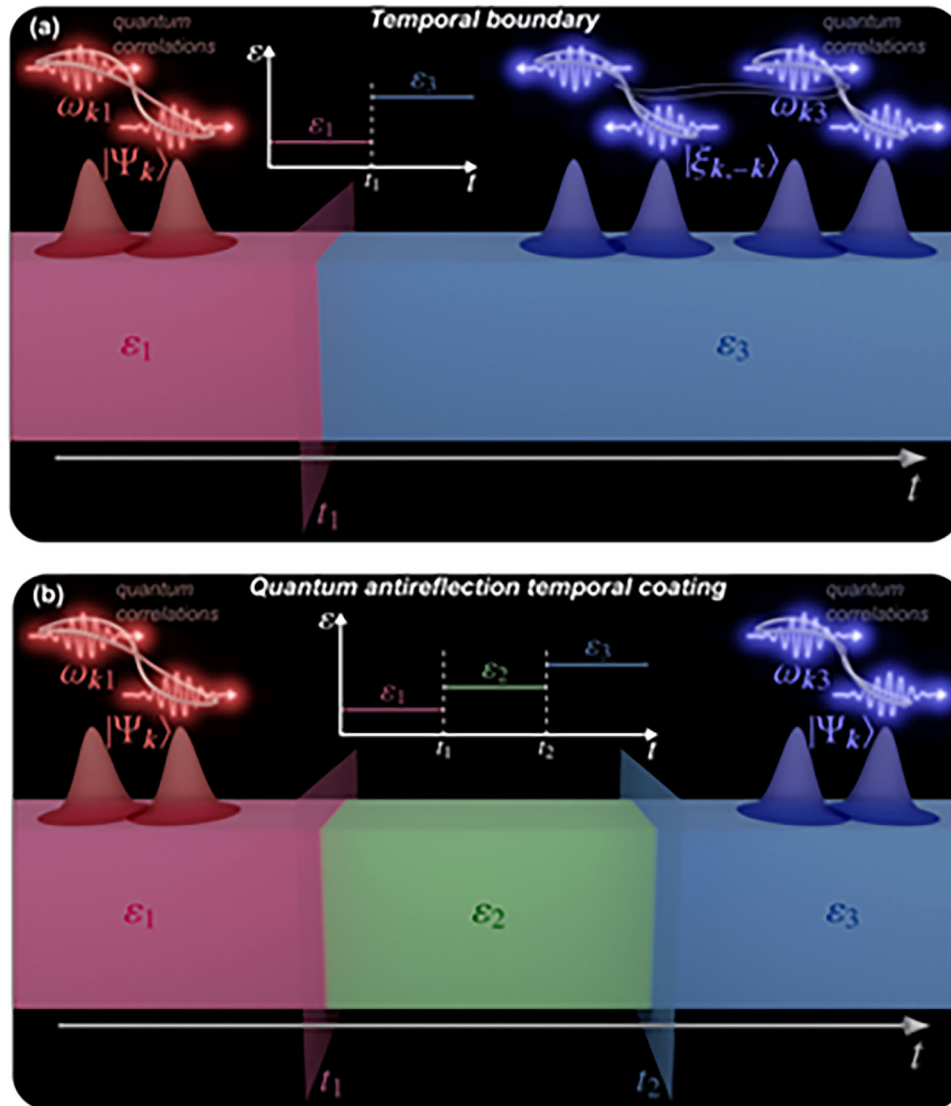
**LASER
& PHOTONICS
REVIEWS**

www.lpr-journal.org

**Figure 1.** Quantum state transformations in temporal boundaries. a) Sketch of the change of a quantum state through a temporal boundary, including the generation of forward and backward photons, with nontrivial quantum correlations between them. b) Quantum ATCs preserve the quantum state, while shifting it in frequency.

theory of quantum state transformations at microwave frequencies is superconducting circuits,[26] where vacuum amplification effects[27] and transmission line metamaterials[28] have been experimentally demonstrated. The implementation of ATCs at optical frequencies is expected to be more challenging as it requires from the ultrafast modulation of the optical properties of a material. However, the actual possibility for realizing temporal metamaterial concepts is spurring a recent upsurge of experiments on ultrafast modulation of optical systems.[29–31]

## 2. Quantum Theory of ATCs

The general structure of an ATC is schematically depicted in **Figure 1**b. It basically consists of two semi-infinite temporal slabs with permittivity $\varepsilon_1$ and $\varepsilon_3$, linked by a temporal matching layer with permittivity $\varepsilon_2$ and duration $\tau = t_2 - t_1$. For simplicity, all

temporal layers are assumed to be nonmagnetic ($\mu_1 = \mu_2 = \mu_3 = 1$).

On each temporal slab, the Hamiltonian of the system is $\hat{H}_n = \sum_k \hbar\omega_{kn}(\hat{a}_{kn}^\dagger \hat{a}_{kn} + 1/2)$, with $n = 1, 2, 3$, representing a continuum of photonic modes with wavevector $\boldsymbol{k}$, frequency $\omega_{kn} = |\mathbf{k}|\, c/\sqrt{\varepsilon_n}$ and destruction operator $\hat{a}_{kn}$. The electric field operator is given by:[17]

$$\widehat{\mathbf{E}}_{kn} = i\sqrt{\frac{\hbar\omega_{kn}}{2\varepsilon_0\varepsilon_n V}}\; \mathbf{e}_{kn}\; e^{i\mathbf{k}\cdot\mathbf{r}}\; \hat{a}_{kn} + h.c. \tag{1}$$

where $V$ is the quantization volume and $\mathbf{e}_{kn}$ is the unit polarization vector. Imposing the continuity of the $\widehat{\mathbf{D}}_{kn}$ and $\widehat{\mathbf{B}}_{kn}$ operators across the temporal boundaries leads to the following

**ADVANCED
SCIENCE NEWS**

www.advancedsciencenews.com

**LASER
& PHOTONICS
REVIEWS**

www.lpr-journal.org

transformation rule for the photonic operators

$$
\begin{aligned}
\hat{a}_{k3} = &\left(\cosh\left(s_{21}\right)\cosh\left(s_{32}\right) + e^{i2\omega_{k2}\tau}\sinh\left(s_{21}\right)\sinh\left(s_{32}\right)\right)\hat{a}_{k1} \\
&- \left(\sinh\left(s_{21}\right)\cosh\left(s_{32}\right) + e^{i2\omega_{k2}\tau}\sinh\left(s_{32}\right)\cosh\left(s_{21}\right)\right)\hat{a}_{-k1}^{\dagger}
\end{aligned}
\tag{2}
$$

where $s_{mn} = \ln\sqrt{Z_m/Z_n}$ is the squeezing parameter characterizing the temporal boundary between the m$^{\text{th}}$ and the n$^{\text{th}}$ temporal slabs, and $Z_m = 1/\sqrt{\varepsilon_m}$ is the medium impedance in the m$^{\text{th}}$ temporal slab. The transformation rule given by Equation (2) has two major characteristics: (i) the combination of forward $\boldsymbol{k}$ and backward $-\boldsymbol{k}$ modes, leading to nontrivial photon correlations between them, and (ii) the mixing of creation and annihilation operators, resulting in photon production and/or absorption effects. For classical waves, the physical meaning of (i) reduces to the generation of forward and backward waves after a temporal sequence. However, from the quantum perspective, it more generally represents the generation of entanglement between different modes, and the change of quantum correlations, in the form of a Bogoliubov transformation. On the other hand, it should be noted that the energy of a classical wave changes when the material parameters are modulated. The mixing of photonic operators pointed out in (ii), forces the presence of creation operators, and generalizes this notion, for example, by including the eventual photon production from the vacuum state. In general, characteristics (i) and (ii) induce a change in the quantum state of the system, as schematically depicted in Figure 1.

For the particular case in which the duration of the temporal slab equals a quarter of the period of the frequency of the mode with wavevector $\boldsymbol{k}$ inside it, i.e., $2\omega_{k2}\tau = \pi$ or $\tau = T_{k2}/4$, the operator transformation rule (2) reduces to

$$
\hat{a}_{k3} = \cosh\left(s_{21} - s_{32}\right)\hat{a}_{k1} - \sinh\left(s_{21} - s_{32}\right)\hat{a}_{-k1}^{\dagger}
\tag{3}
$$

In other words, a $T_{k2}/4$ temporal slab results in a two-mode squeezing transformation, where the effective squeezing parameter is the subtraction of the squeezing parameter for the first and second temporal boundaries composing the temporal slab. Equivalently, it can be stated that the impact of a $T_{k2}/4$ temporal slab is that of a single temporal boundary, with effective squeezing parameter $s_{21} - s_{32}$.

In view of Equation (3), it is clear that a case of particular interest will be $s_{21} - s_{32} = 0$, that is, when the squeezing parameters of the first and second temporal boundaries exactly cancel out. As $s_{mn} = \ln\sqrt{Z_m/Z_n}$, it can be readily checked that this condition is equivalent to $Z_2 = \sqrt{Z_1 Z_3}$; that is, the impedance of the matching layer should equal the geometric mean of the initial and final medium impedances. This condition is exactly equivalent to that of a classical $T/4$ ATC[10] or a traditional $\lambda/4$ impedance matching network in the spatial domain.[11] In such a case, the operator transformation rule for an ATC simply reduces to:

$$
\hat{a}_{k3} = \hat{a}_{k1}
\tag{4}
$$

This simple relation between the operators before and after the temporal slab has a clear physical meaning: Quantum states are projected with no changes in their photon statistics, preserving all their quantum correlations. At the same time, the frequency of the photonic modes is shifted from $\omega_{k1} = |\boldsymbol{k}|\,c/\sqrt{\varepsilon_1}$ to $\omega_{k3} = |\boldsymbol{k}|\,c/\sqrt{\varepsilon_3}$ (after applying the second temporal boundary at $t = t_2$). Therefore, an ATC allows for a quantum state to be perfectly transferred through a temporal sequence, while shifting it in frequency.

Here, it is worth remembering that the ATC is composed by two temporal boundaries where photon creation/annihilation processes take place. At the same time, an ATC is precisely designed such that the photon creation/annihilation processes in both temporal boundaries are canceled out. Thus, all photon creation/annihilation processes are effectively cancelled out at an ATC, and the quantum response is exactly that of a pure frequency shift. We note that a similar pure frequency shift could be obtained with a slow process such as an adiabatic taper.[32] The advantage of an ATC is that it operates at a much faster time scale, that is, one quarter of the period. Naturally, such dramatic reduction in the time of operation must come at a cost, and ATCs operate within a limited bandwidth, as it is illustrated in the examples below.

As high quality quantum sources are typically restricted to a set of specific wavelengths, quantum frequency conversion is a major technological challenge in the current development of quantum technologies.[33–38] In particular, frequency shifting nonclassical light states is required to operate at frequencies where propagation losses are small, to fully exploit the bandwidth, to develop tunable nonclassical light sources, or to connect with other elements of the photonic network such as a quantum memory. Our analysis on the quantum response reveals that ATCs might be of interest as they provide a fast frequency shifting procedure, a process only taking the duration of the matching layer, that is, a quarter of the period within it.

## 3. Revisiting the Classical Case

Next, we use the quantum formalism to revisit and bring new insights into the classical response of ATCs.[10] To represent a classical wave, we set the initial state of the system as a coherent state $|\psi_{\text{in}}\rangle = \hat{D}_{k1}(\alpha)|0\rangle$, where $\hat{D}_{k1}(\alpha) = \exp(\alpha\hat{a}_{k1}^{\dagger} - \alpha^*\hat{a}_{k1})$ is the displacement operator with complex amplitude $\alpha = \alpha' + i\alpha''$.[17] The configuration is schematically depicted in **Figure 2**a.

As anticipated, the major feature of a quantum ATC is that it preserves the quantum state and all its photon statistics; that is to say, the average number of photons $\langle n_{k1}\rangle = \langle n_{k3}\rangle = |\alpha|^2$, the amplitude $\langle X_{k1} + iY_{k1}\rangle = \alpha = \langle X_{k3} + iY_{k3}\rangle$, and the variances $\Delta X_{k1}^2 = \Delta Y_{k1}^2 = \frac{1}{4} = \Delta X_{k3}^2 = \Delta Y_{k3}^2$ of the quadrature operators, $X_{kn} = (\hat{a}_{kn}^{\dagger} + \hat{a}_{k1})/\sqrt{2}$ and $Y_{kn} = i(\hat{a}_{kn}^{\dagger} - \hat{a}_{k1})/\sqrt{2}$, as well as any other photon statistic will remain those of the initial coherent state (see **Figure 3**a).

At the same time, preserving photon statistics does not imply that all physical quantities will remain invariant. Up and down frequency conversion takes place according to the ratio: $\omega_{k3}/\omega_{k1} = \sqrt{\varepsilon_1/\varepsilon_3}$. Similarly, the energy of the system scales from $\langle\hat{H}_{k1}\rangle = \hbar\omega_{k1}|\alpha|^2$ to $\langle\hat{H}_{k3}\rangle = \hbar\omega_{k3}|\alpha|^2$, directly following the frequency change (see Figure 2b). This means that switching to a higher permittivity value $\varepsilon_3 > \varepsilon_1$ leads to a smaller frequency $\omega_{k3} < \omega_{k1}$, and a smaller energy $\langle\hat{H}_{k3}\rangle < \langle\hat{H}_{k1}\rangle$. Such inverse relation between energy and permittivity change is also consistent
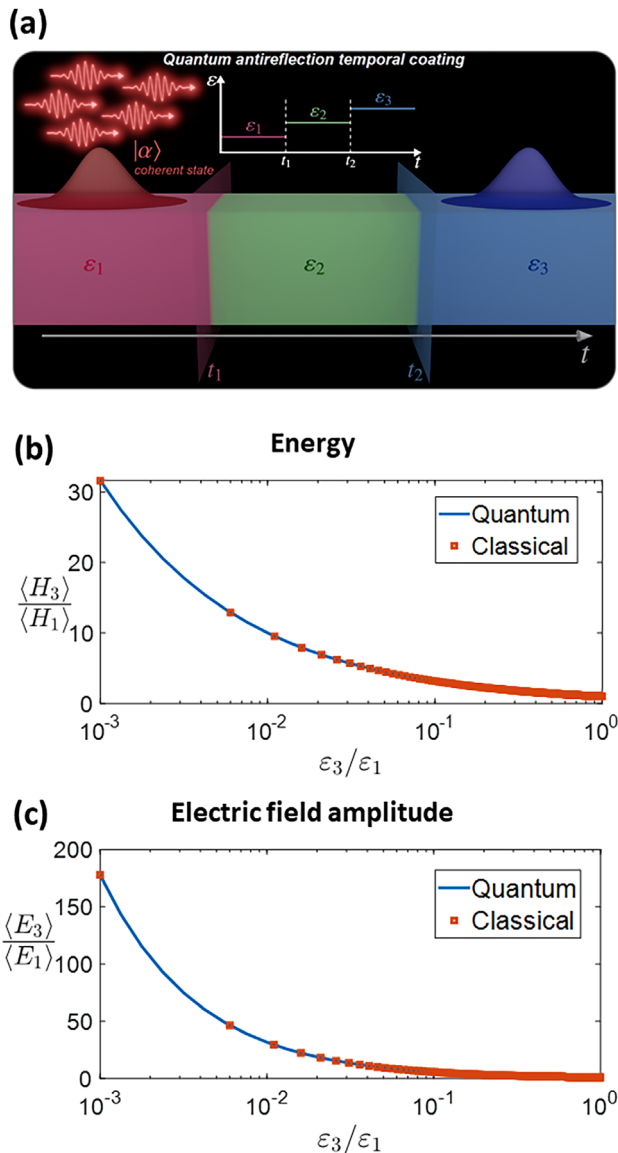
**Figure 2.** Revisiting the classical response of a ATC. a) Sketch of a quantum ATC excited with a "classical" coherent state $|\alpha\rangle$. Change in the b) energy and c) electric field amplitude as a function of the permittivity contrast. Comparison with the classical prediction of the energy and electric field amplitude, calculated following refs. [10, 12] shows an excellent agreement. Note that the results for the $\varepsilon_3/\varepsilon_1 > 1$ range would simply be the inverse of these results.

with the classical energy $H_n = \int dV\, (\mathbf{D}^2(\mathbf{r}, t)/\varepsilon_n + \mathbf{B}^2(\mathbf{r}, t)/\mu_0)$ , which, in combination with the continuity of the $\mathbf{D}(\mathbf{r}, t)$ and $\mathbf{B}(\mathbf{r}, t)$ fields at the time when the permittivity is changed, indicates that an increase of the dielectric permittivity is associated with a decrease of the energy of the electromagnetic field. Likewise, as shown in Figure 2c, the amplitude of the electric field changes following a $\langle \hat{E}_{k3} \rangle / \langle \hat{E}_{k1} \rangle = (\varepsilon_1/\varepsilon_3)^{3/4}$ scaling factor, in accordance to the $\sqrt{\omega_{kn}/\varepsilon_n}$ prefactor of the electric field operator in Equation (1). These scaling factors are consistent with recent discussions on the operation principle of classical ATCs and the ex-

tent of their analogy with spatial matching layers.[12] In fact, panels (b) and (c) in Figure 2 also include, respectively, a numerical calculation for the classical prediction of the change in the energy and the electric field amplitude, showing an excellent agreement.

It is worth remarking that, for most temporal boundaries, the quantum and classical predictions of the change in the energy do not necessarily match due to the amplification of the quantum noise in coherent states. However, this effect is inhibited in quantum ATCs; so that, the output energy predicted by the classical and quantum theories matches, as shown in Figure 2. In order to illustrate this point, in **Figure 4**, we depict the frequency response of the average value of the energy in the forward wave for attenuated coherent states with a small number of photons. It can be observed that, in general, the quantum and classical predictions of the energy do not match due to the photons produced via vacuum amplifications effects. At the same time, at the frequency where the system operates as an ATC, the predictions of the quantum and classical theories perfectly agree in all cases due to the inhibition of vacuum amplification effects.

Thus, we find that the classical theory of ATCs fails even for "classical" coherent states when these are strongly attenuated into the few photon regime ($|\alpha|^2 = 0.25$, see Figure 4a). At the same time, we note that the differences apparently vanish for coherent states with a sufficiently large number of photons ($|\alpha|^2 = 10$, see Figure 4c). When the energy of the incident wave increases, the modifications on the energy introduced by vacuum amplification effects are comparatively small, and the predictions of quantum and classical theories eventually overlap. By contrast, classical and quantum predictions perfectly match at the ATC frequency in all regimes because the quantum state is shifted in frequency without the addition of quantum noise.

Hence, the quantum theory provides a more complete picture of the operational principle of ATCs: quantum states are perfectly transferred through them, with no changes in their photon statistics. Thus, all the observed differences in the properties of the classical waves before and after the ATC are justified by the fact that, for a different background medium, each quanta of light has a different energy and a different electric field strength.

Finally, we emphasize that, from the quantum theory perspective, the impact of an unmatched temporal boundary goes beyond the mere generation of a backward wave. If we were to switch between media 1 and 3 without the temporal matching layer (i.e., using a simple temporal boundary), the operator transformation rule would be that of a single temporal boundary: $\hat{a}_{k3} = \cosh(s_{31})\,\hat{a}_{k1} - \sinh(s_{31})\hat{a}_{-k1}^\dagger$. Consequently, there would be changes in the output photon statistics for both the forward and backward waves, including the amplitude of the quadrature operators $\langle X_{k3} + iY_{k3}\rangle = \alpha_{k3} = \cosh(s_{31})\alpha$ and $\langle X_{-k3} + iY_{-k3}\rangle = \alpha_{-k3} = -\sinh(s)\alpha^*$, the average number of photons, $\langle n_{k3} \rangle = |\alpha_{sk3}|^2 + \sinh^2(s_{31})$ and $\langle n_{-k3} \rangle = |\alpha_{-k3}|^2 + \sinh^2(s_{31})$, and the variances $\Delta X_{k3}^2 = \Delta Y_{k3}^2 = \Delta X_{-k3}^2 = \Delta Y_{-k3}^2 = \frac{1}{4}\cosh(2s)$ (compare Figure 3a,c).

In addition, the existence of a backward wave imposes non-trivial photon correlations that cannot be appreciated under a classical approach. To illustrate this point, we recast the photonic
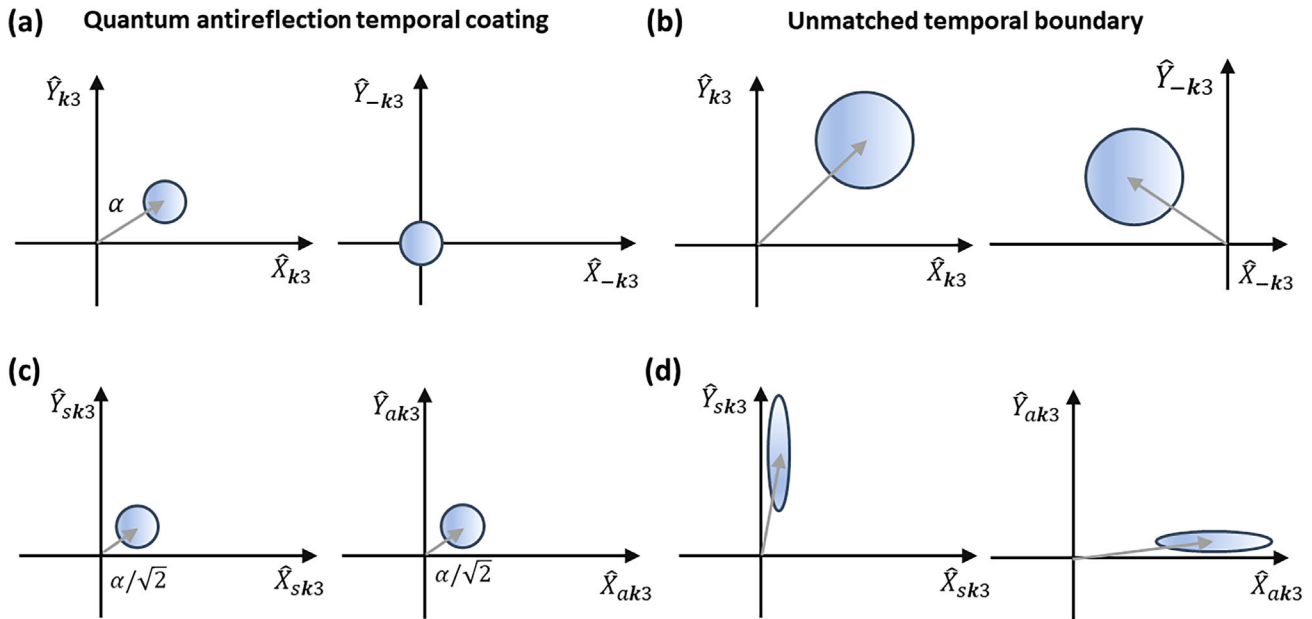
**ADVANCED
SCIENCE NEWS**

www.advancedsciencenews.com

LASER
& PHOTONICS
REVIEWS

www.lpr-journal.org

**Figure 3.** Photon statistics after the transformation of a coherent state. Sketch of the magnitude and variance of the quadrature operators in the a,b) forward/backward and c,d) symmetric/antisymmetric basis, after a quantum ATC (a,c) and an unmatched temporal boundary (b,d). The figure illustrates how an unmatched temporal boundary qualitatively changes the photon statistics of a "classical wave," while a quantum ATC preserves the photon statistics of a coherent state.

operators in a basis formed by symmetric $\hat{a}_{sk} = (\hat{a}_k + \hat{a}_{-k})/\sqrt{2}$ and antisymmetric $\hat{a}_{ak} = (\hat{a}_k - \hat{a}_{-k})/\sqrt{2}$ operators, which makes more evident the squeezing nature of the transformation. In this basis, the amplitude of the quadrature operator changes from $\langle X_{sk1} + iY_{sk1}\rangle = \alpha/\sqrt{2} = \langle X_{ak1} + iY_{ak1}\rangle$ to $\langle X_{sk3} + iY_{sk3}\rangle = \alpha_{a3} = \frac{1}{\sqrt{2}}(e^{-s_{31}}\alpha' + i\,e^{s_{31}}\alpha'')$ and to $\langle X_{ak3} + iY_{ak3}\rangle = \alpha_{a3} = \frac{1}{\sqrt{2}}(e^{s_{31}}\alpha' + i\,e^{-s_{31}}\alpha'')$, as shown in Figure 3. Similarly, the number of photons changes from $\langle n_{sk1}\rangle = \langle n_{ak1}\rangle = |\alpha|^2/2$ to $\langle n_{sk3}\rangle = |\alpha_{s3}|^2 + \sinh^2(s_{31})$ and $\langle n_{ak3}\rangle = |\alpha_{a3}|^2 + \sinh^2(s_{31})$, and the variances of the quadrature operators change from $\Delta X_{sk1}^2 = \Delta Y_{sk1}^2 = \Delta X_{ak1}^2 = \Delta Y_{ak1}^2 = 1/4$ to $\Delta X_{sk1}^2 = \Delta Y_{ak1}^2 = \frac{1}{4}e^{-2s_{31}}$ and $\Delta Y_{sk1}^2 = \Delta X_{ak1}^2 = \frac{1}{4}e^{2s_{31}}$ (see Figure 3).

In conclusion, from the quantum theory perspective, the impact of an unmatched temporal boundary is not limited to generating a reflected wave. It changes the photon statistics and generates nontrivial quantum correlations between the forward and backward waves in the form of a two-mode squeezing transformation. ATCs solve this problem, not only inhibiting the generation of a backward wave but by preserving all photon statistics while shifting the frequency of the quantum state.

## 4. Thermal Fields and Fast Switching With Suppressed Noise

Aside from quantum vacuum amplification effects, it is expected that temporal boundaries should also result in the amplification of thermal field fluctuations. This effect is of more practical relevance because the generation of additional thermal noise would degrade the performance of any communication, sensing,

or computation technology based on time-varying media.[39,40] On the other hand, control over radiative thermal noise generation can be harnessed for heat and energy management,[41,42] as well as for nanophotonic thermal engines.[43] In this section, we show that ATCs allow for ultra-fast switching with reduced thermal noise generation.

To illustrate this point, we consider a material body at thermal equilibrium with a background environment at temperature $T_e$ (see **Figure 5**). In such scenario, the optical modes are thermally populated, which can be described through the following density matrix:[17]

$$\hat{\rho}_{th} = \otimes_k \left(1 - e^{-\beta_{k1}}\right) \sum_{n_{k1}=0}^{\infty} e^{-\beta_{k1}n_{k1}}|n_{k1}\rangle\langle n_{k1}| \tag{5}$$

with $\beta_{k1} = \hbar\omega_{k1}/k_B T_e$. Consequently, the average number of photons populating the modes is $\langle n_{k1}\rangle = (e^{\beta_{k1}} - 1)^{-1}$, and the variances of the quadrature operators are $\Delta X_{k1}^2 = \Delta Y_{k1}^2 = \frac{1}{4}(1 + 2\langle n_{k1}\rangle)$.

Assume that we wish to rapidly switch in time the permittivity of the medium from $\varepsilon_1$ to $\varepsilon_3$, a process that can be modelled by a single temporal boundary, with transformation rule $\hat{a}_{k3} = \cosh(s_{31})\hat{a}_{k1} - \sinh(s_{31})\hat{a}_{-k1}^\dagger$. It is expected that the interaction of the temporal boundary with the thermal fields will lead to amplification effects of the thermal noise. Specifically, the average number of photons after the temporal boundary is $\langle n_{k3}\rangle = \langle n_{k1}\rangle\cosh^2(s_{31}) + \sinh^2(s_{31})$. The first term corresponds to the amplification of the thermal noise. The second term comes from a quantum vacuum amplification effect, akin to the dynamical Casimir effect.[27,44] We note that the number of photons always increases, independently of whether the final permittivity
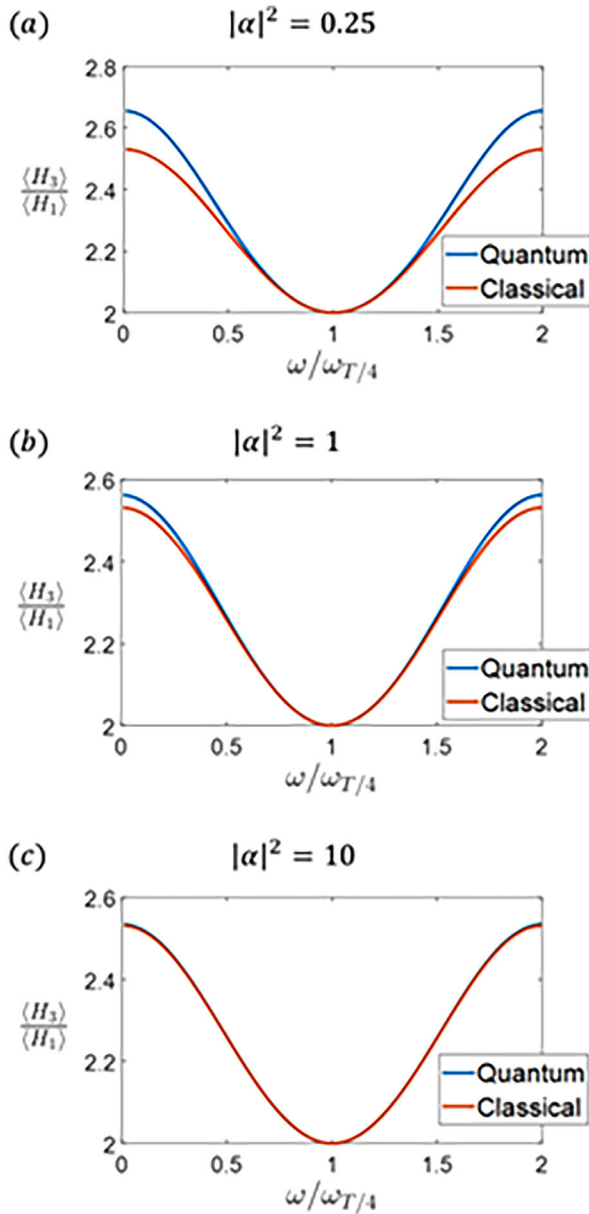
# ADVANCED
## SCIENCE NEWS

www.advancedsciencenews.com

www.lpr-journal.org

LASER
& PHOTONICS
REVIEWS

**Figure 4.** Frequency response for attenuated coherent states. Comparison between the classical and quantum predictions for the average energy value, normalized to the input energy, for an ATC with $\varepsilon_1 = 4$, $\varepsilon_2 = 2$, and $\varepsilon_3 = 1$, and for attenuated coherent states with a) less than one photon in average, $|\alpha|^2 = 0.25$; b) one photon in average, $|\alpha|^2 = 1$; and c) ten photons in average, $|\alpha|^2 = 10$.

value is smaller $\varepsilon_3 < \varepsilon_1$ or larger $\varepsilon_3 > \varepsilon_1$ than the original one. The larger the permittivity contrast, the larger the photon production is. Similarly, the variances of the quadrature operators increase to $\Delta X_{k3}^2 = \Delta Y_{k3}^2 = \frac{1}{4}(1 + 2\sinh^2(s_{31}) + 2\langle n_{k1}\rangle \cosh^2(2s_{31}))$.

Our analysis confirms that the interaction between thermal fields and the switching mechanism entails the amplification of thermal noise. In turn, this additional noise will have a detrimen-

tal impact on the performance of the system. For example, amplifying thermal fields effectively increases the noise temperature of the system and it will lead to spurious photon counts on detectors located outside the material system. In addition, the amplification of the thermal fields implies that the energy of the electromagnetic system is increased. In short, the larger the noise of the system, the larger the amount of energy that must be pumped into it, negatively affecting the energy efficiency of the switching process.

ATCs, however, have the ability to mitigate the amplification of thermal noise. As the transformation rule reduces to $\hat{a}_{k3} = \hat{a}_{k1}$, the thermal state is preserved, including the average number of photons, the variances of the quadrature operators, and any other photon statistic. Thus, ATCs make it possible to rapidly switch the system without amplifying the thermal noise. The cost is to reduce the speed of the process to a quarter period (with respect to the frequency associated with the mode of interest within the temporal matching layer).

In order to illustrate this effect, we compare the average thermal spectral energy density before and after the permittivity of the system has been switched from $\varepsilon_1 = 1$ to $\varepsilon_3 = 4$, for three different mechanisms: instantaneous switching (see **Figure 6**a), a quarter-period ATC (see Figure 6b), and a fourth-order binomial ATC (see Figure 6c). We assume that the system is initially at thermal equilibrium at temperature $T_1 = 300$ K, with average spectral energy density $\langle \hat{H}_{k1}\rangle = \hbar\omega_{k1}(e^{\beta_{k1}} - 1)^{-1}$ with the low-frequency limit $\langle \hat{H}_{k1}\rangle \approx k_B T_1$ (see Figure 6a). If the system is instantaneously switched from $\varepsilon_1$ to $\varepsilon_3$, the spectral energy density increases to $\langle \hat{H}_{k3}\rangle = \hbar\omega_{k3}[\cosh^2(s_{31})(e^{\beta_{k1}} - 1)^{-1} + \sinh^2(s_{31})]$. For non-cryogenic temperatures and in the low frequency limit, the spectral energy can be approximated by $\langle \hat{H}_{k3}\rangle \approx k_B[\cosh^2(s_{31})T_1]$, which can be understood as an effective increase of the temperature to $T_3 = \cosh^2(s_{31})T_1$, as shown in Figure 6a.

Next, we assume that the system is switched following a quarter-period ATC, with parameters $\varepsilon_2 = \sqrt{\varepsilon_1\varepsilon_3}$, $\tau = T_0/4 \times \sqrt{\varepsilon_2}$ and $T_0 = 0.1$ ns, designed for an operating frequency of 10 GHz. While the choice of the frequency of operation is illustrative, in view of experimental demonstrations of ATCs and photonic time crystals at RF and microwave frequencies,[24,25] as well as the possible implementation of low-temperature quantum and thermal noise effects with superconducting circuits,[26–28] it has been selected in the microwave regime. It can be concluded from Figure 6b that the addition of the ATC induces a periodical response, related to the phase evolution through it, while keeping an overall reduction of the amplification of the thermal noise. In fact, it can be seen that the spectral density approximately follows an oscillatory behavior between the $k_B T_1$ and $k_B[\cosh^2(s_{31})T_1]$ limits, and that the amplification is exactly zero at the frequency of operation.

We note that a further suppression of thermal noise generation would be obtained with more sophisticated switching mechanisms. To illustrate this point, we implement an "impedance transformer" consisting of the fourth-order binomial ATC design presented in ref. [15]. The temporal sequence consists of four temporal layers with parameters: $\varepsilon_a = 1.09$, $\varepsilon_b = 1.54$, $\varepsilon_c = 2.59$, $\varepsilon_d = 3.67$; and $\tau_a = 1.09$, $\tau_b = 1.54$, $\tau_c = 2.59$, and $\tau_d = 3.67$.[15]
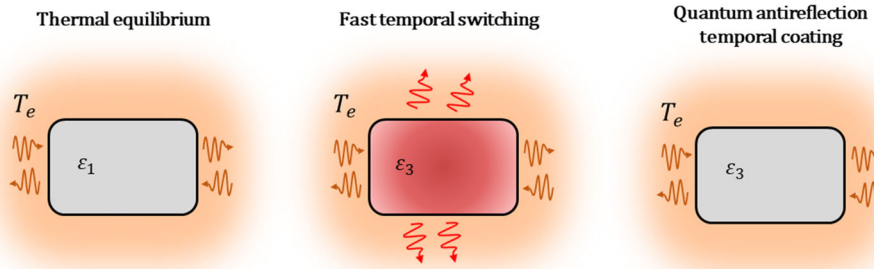
**ADVANCED
SCIENCE NEWS**

www.advancedsciencenews.com

**LASER
& PHOTONICS
REVIEWS**

www.lpr-journal.org

**Figure 5.** Inhibiting thermal noise amplification during fast switching. (Left) A system characterized by relative permittivity $\varepsilon_1$ being at thermal equilibrium with a background at temperature $T_e$. (Center) Amplification of thermal fields after fast switching the permittivity of the body to $\varepsilon_3$. (Right) Inhibition of thermal noise amplification by a quantum ATC.

For an N-layered temporal sequence, the quantum input–output relations can be written in the following transfer matrix form:[19]

$$\begin{bmatrix} \hat{a}_{kN} \\ \hat{a}^{\dagger}_{-kN} \end{bmatrix} = S\left(s_{NN-1}\right) U\left(\varphi_{N-1}\right) S\left(s_{N-1N-2}\right) \cdots U\left(\varphi_2\right) S\left(s_{21}\right) \begin{bmatrix} \hat{a}_{k1} \\ \hat{a}^{\dagger}_{-k1} \end{bmatrix}$$

(6)

with the squeezing matrix

$$S(s) = \begin{bmatrix} \cosh(s) & -\sinh(s) \\ -\sinh(s) & \cosh(s) \end{bmatrix}$$

(7)

and the time evolution matrix

$$U(\varphi_n) = \begin{bmatrix} e^{-i\varphi_n} & 0 \\ 0 & e^{i\varphi_n} \end{bmatrix}$$

(8)

with the phase advance $\varphi_n = \omega_{kn} \tau_n$. The numerical results presented in Figure 6c confirm that the overall amplification of thermal noise is further reduced with the binomial ATC by flattening the minima of the spectral energy density. It is also found that the spectral energy density never surpasses the $k_B[\cosh^2(s_{31})T_1]$

limit at any frequency. Thus, it is confirmed that advanced ATCs enable a stronger inhibition of thermal noise generation. At the same time, it is worth remarking that this reduction in thermal noise generation is obtained at the cost of increasing the switching time. Ultimately, one could totally suppress all thermal noise amplification by extending the switching time into the adiabatic regime. At any rate, ATCs offer the possibility of designing temporal sequences that minimize thermal noise generation in a frequency band of interest and for a given restriction of the switching time.

## 5. Conclusion

Our results highlight the importance of investigating the quantum optical response of time-varying media. By studying the quantum response of ATCs, we were able to provide a clearer perspective of their classical operating principle, bringing a fresh perspective to recent studies. In addition, our formalism suggested two new potential applications of ATCs: quantum frequency shifting for photonic quantum networks and fast material switching without the amplification of thermal fields in the system. We expect that our results will motivate further research
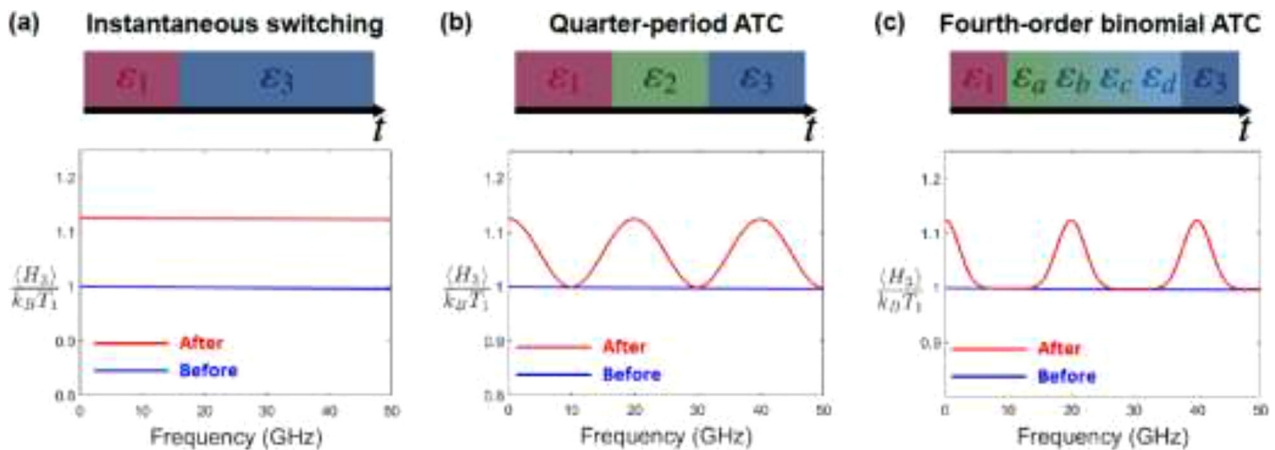


**Figure 6.** Comparison of the average thermal spectral energy density before and after different fast switching mechanisms. a) Instantaneous switching from $\varepsilon_1 = 1$ to $\varepsilon_3 = 4$. b) A quarter-period ATC, with $\varepsilon_2 = \sqrt{\varepsilon_1\varepsilon_3}$ and $\tau = T_0/4 \times \sqrt{\varepsilon_2}$ with $T_0 = 0.1$ ns for an operating frequency of 10 GHz. c) A fourth order binomial ATC with parameters $\varepsilon_a = 1.09$, $\varepsilon_b = 1.54$, $\varepsilon_c = 2.59$, $\varepsilon_d = 3.67$; $\tau_a = 1.09$, $\tau_b = 1.54$, $\tau_c = 2.59$, and $\tau_d = 3.67$ as extracted from ref. [15]. Note that the average energy of the forward propagating mode is normalized to the low-frequency limit $k_B T_1$, for a system initially at thermal equilibrium at temperature $T_1$.

ADVANCED
SCIENCE NEWS

www.advancedsciencenews.com

LASER
& PHOTONICS
REVIEWS

www.lpr-journal.org

in the field, combining quantum optics and time-varying media. For example, our results could be extended to more sophisticated ATCs based on multilayered media, which could provide for control over the spectral response.

## Conflict of Interest

The authors declare no conflict of interest.

## Data Availability Statement

The data that support the findings of this study are available from the corresponding author upon reasonable request.

[1] S. Yin, E. Galiffi, A. Alù, *eLight* **2022**, *2*, 8.
[2] E. Galiffi, R. Tirole, S. Yin, H. Li, S. Vezzoli, P. A. Huidobro, M. G. Silveirinha, R. Sapienza, A. Alù, J. B. Pendry, *Adv. Photonics* **2022**, *4*, 014002.
[3] C. Caloz, Z.-L. Deck-Léger, *IEEE Trans. Antennas Propag.* **2020**, *68*, 1583.
[4] N. Engheta, *Nanophotonics* **2021**, *10*, 639.
[5] G. Ptitcyn, M. S. Mirmoosa, S. A. Tretyakov, *Phys. Rev. Res.* **2019**, *1*, 023014.
[6] F. R. Morgenthaler, *IRE Trans. Microwave Theory Tech.* **1956**, *6*, 167.
[7] R. L. Fante, *IEEE Trans. Antennas Propag.* **1971**, *19*, 417.
[8] V. Bacot, M. Labousse, A. Eddi, M. Fink, E. Fort, *Nat. Phys.* **2016**, *12*, 972.
[9] S. Yin, A. Alù, *ACS Photonics* **2022**, *9*, 979.
[10] V. Pacheco-Peña, N. Engheta, *Optica* **2020**, *7*, 323.
[11] D. M. Pozar, *Microwave Engineering*, 4th ed., John Wiley & Sons, Hoboken, NJ **2009**.
[12] V. Pacheco-Peña, N. Engheta, *Optica* **2021**, *8*, 826.
[13] W. Mai, J. Xu, D. H. Werner, *Optica* **2021**, *8*, 824.
[14] D. Ramaccia, A. Alù, A. Toscano, F. Bilotti, *Appl. Phys. Lett.* **2021**, *118*, 101901.
[15] G. Castaldi, V. Pacheco-Peña, M. Moccia, N. Engheta, V. Galdi, *Nanophotonics* **2021**, *10*, 3687.
[16] Y. Zhang, L. Peng, J. Wang, D. Ye, *Opt. Express* **2022**, *323*, 40357.
[17] R. Loudon, *The Quantum Theory of Light*, Oxford University Press, Oxford, UK **2000**.
[18] M. O. Scully, M. S. Zubairy, *Quantum Optics*, Cambridge University Press, Cambridge, UK **1997**.
[19] J. E. Vázquez-Lozano, I. Liberal, *Nanophotonics* **2022**, *12*, 539.
[20] J. T. Mendonça, A. Guerreiro, A. M. Martins, *Phys. Rev. A* **2000**, *62*, 033805.
[21] J. B. Pendry, E. Galiffi, P. A. Huidobro, *Optica* **2022**, *9*, 724.
[22] M. Lyubarov, Y. Lumer, A. Dikopoltsev, E. Lustig, Y. Sharabi, M. Segev, *Science* **2022**, *3324*, 2003.
[23] A. Dikopoltsev, Y. Sharabi, M. Lyubarov, Y. Lumer, S. Tsesses, E. Lustig, I. Kaminer, M. Segev, *Proc. Natl. Acad. Sci. U. S. A.* **2022**, *119*, e2119705119.
[24] H. Moussa, G. Xu, S. Yin, E. Galiffi, Y. Radi, A. Alù, *Nat. Phys.* **2022**, *19*, 863.
[25] J. R. Reyes-Ayona, P. Halevi, *Appl. Phys. Lett.* **2015**, *107*, 074101.
[26] X. Gu, A. F. Kockum, A. Miranowicz, Y. xi Liu, F. Nori, *Phys. Rep.* **2017**, *718–719*, 1.
[27] P. D. Nation, J. R. Johansson, M. P. Blencowe, F. Nori, *Rev. Mod. Phys.* **2012**, *84*, 1.
[28] M. Mirhosseini, E. Kim, V. S. Ferreira, M. Kalaee, A. Sipahigil, A. J. Keller, O. Painter, *Nat. Commun.* **2018**, *9*, 3706.
[29] Y. Zhou, M. Z. Alam, M. Karimi, J. Upham, O. Reshef, C. Liu, A. E. Willner, R. W. Boyd, *Nat. Commun.* **2020**, *11*, 2180.
[30] J. Bohn, T. S. Luk, S. Horsley, E. Hendry, *Optica* **2021**, *8*, 1532.
[31] R. Tirole, S. Vezzoli, E. Galiffi, I. Robertson, D. Maurice, B. Tilmann, S. A. Maier, J. B. Pendry, R. Sapienza, *Nat. Phys.* **2023**, 1.https://doi.org/10.1038/s41567-023-01993-w
[32] E. Galiffi, S. Yin, A. Alú, *Nanophotonics* **2022**, *11*, 3575.
[33] B. Da Lio, C. Faurby, X. Zhou, M. L. Chan, R. Uppu, H. Thyrrestrup, S. Scholz, A. D. Wieck, A. Ludwig, P. Lodahl, L. Midolo, *Adv. Quantum Technol.* **2022**, *5*, 2200006.
[34] R. Ikuta, Y. Kusaka, T. Kitano, H. Kato, T. Yamamoto, M. Koashi, N. Imoto, *Nat. Commun.* **2011**, *2*, 537.
[35] J. T. Hill, A. H. Safavi-Naeini, J. Chan, O. Painter, *Nat. Commun.* **2012**, *3*, 1196.
[36] J. Huang, P. Kumar, *Phys. Rev. Lett.* **1992**, *68*, 2153.
[37] S. Zaske, A. Lenhard, C. A. Keßler, J. Kettler, C. Hepp, C. Arend, R. Albrecht, W. M. Schulz, M. Jetter, P. Michler, C. Becher, *Phys. Rev. Lett.* **2012**, *109*, 147404.
[38] S. Tanzilli, W. Tittel, M. Halder, O. Alibart, P. Baldi, N. Gisin, H. Zbinden, *Nature* **2005**, *437*, 116.
[39] S. W. Wedge, D. B. Rutledge, *IEEE Microwave Guided Wave Lett.* **1991**, *1*, 117.
[40] H. A. Haus, *IEEE J. Quantum Electron.* **2001**, *37*, 813.
[41] A. P. Raman, M. A. Anoma, L. Zhu, E. Rephaeli, S. Fan, *Nature* **2014**, *515*, 540.
[42] S. V. Boriskina, H. Zandavi, B. Song, Y. Huang, G. Chen, *Opt. Photonics News* **2017**, *28*, 26.
[43] D. Gelbwaser-Klimovsky, N. Graham, M. Kardar, M. Kruger, *Phys. Rev. Lett.* **2021**, *126*, 170401.
[44] V. Dodonov, *Physics* **2020**, *2*, 67.